Journal Pre-proof

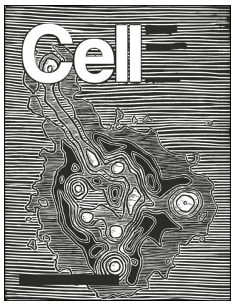

SARS-CoV-2 variants B.1.351 and P.1 escape from neutralizing antibodies

Markus Hoffmann, Prerna Arora, Rüdiger Groß, Alina Seidel, Bojan F. Hörnich, Alexander S. Hahn, Nadine Krüger, Luise Graichen, Heike Hofmann-Winkler, Amy Kempf, Martin S. Winkler, Sebastian Schulz, Hans-Martin Jäck, Bernd Jahrsdörfer, Hubert Schrezenmeier, Martin Müller, Alexander Kleger, Jan Münch, Stefan Pöhlmann

PII: S0092-8674(21)00367-6

DOI: https://doi.org/10.1016/j.cell.2021.03.036

Reference: CELL 11954

To appear in: *Cell*

Received Date: 11 February 2021

Revised Date: 26 February 2021

Accepted Date: 16 March 2021

Please cite this article as: Hoffmann, M., Arora, P., Groß, R., Seidel, A., Hörnich, B.F., Hahn, A.S., Krüger, N., Graichen, L., Hofmann-Winkler, H., Kempf, A., Winkler, M.S., Schulz, S., Jäck, H.-M., Jahrsdörfer, B., Schrezenmeier, H., Müller, M., Kleger, A., Münch, J., Pöhlmann, S., SARS-CoV-2 variants B.1.351 and P.1 escape from neutralizing antibodies, *Cell* (2021), doi: https://doi.org/10.1016/j.cell.2021.03.036.

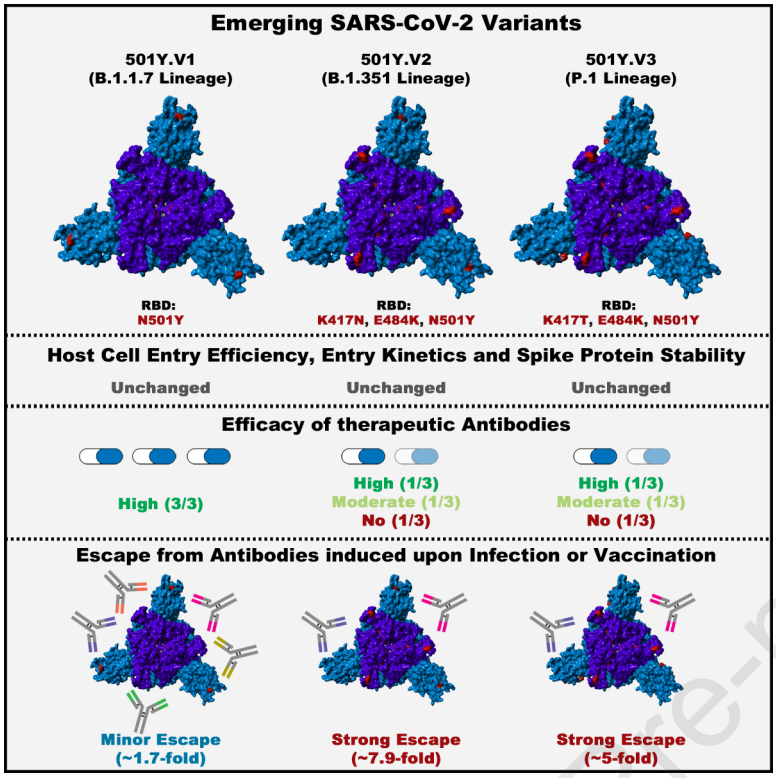

SARS-CoV-2 variants B.1.351 and P.1 escape from neutralizing antibodies

Markus Hoffmann[1,2,11,*], Prerna Arora[1,2,11], Rüdiger Groß[3,11], Alina Seidel[3,11], Bojan F. Hörnich[4], Alexander S. Hahn[4], Nadine Krüger[1], Luise Graichen[1], Heike Hofmann-Winkler[1], Amy Kempf[1,2], Martin S. Winkler[5], Sebastian Schulz[6], Hans-Martin Jäck[6], Bernd Jahrsdörfer[7,8], Hubert Schrezenmeier[7,8], Martin Müller[9], Alexander Kleger[9], Jan Münch[3,10], Stefan Pöhlmann[1,2,12,*]

[1]*Infection Biology Unit, German Primate Center, Kellnerweg 4, 37077 Göttingen, Germany*
[2]*Faculty of Biology and Psychology, Georg-August-University Göttingen, Wilhelmsplatz 1, 37073 Göttingen, Germany*
[3]*Institute of Molecular Virology, Ulm University Medical Center, Meyerhofstr. 1, 89081 Ulm, Germany*
[4]*Junior Research Group Herpesviruses - Infection Biology Unit, German Primate Center, Kellnerweg 4, 37077 Göttingen, Germany*
[5]*Department of Anaesthesiology, University of Göttingen Medical Center, Göttingen, Georg-August University of Göttingen, Robert-Koch-Straße 40, 37075 Göttingen, Germany*
[6] *Division of Molecular Immunology, Department of Internal Medicine 3, Friedrich-Alexander University of Erlangen-Nürnberg, Glückstraße 6, 91054 Erlangen, Germany*
[7]*Department of Transfusion Medicine, Ulm University, Helmholtzstraße 10, 89081 Ulm, Germany*
[8]*Institute for Clinical Transfusion Medicine and Immunogenetics, German Red Cross Blood Transfusion Service Baden-Württemberg – Hessen and University Hospital Ulm, Helmholtzstraße 10, 89081 Ulm, Germany*
[9]*Department of Internal Medicine 1, Ulm University Hospital, Albert-Einstein-Allee 23, 89081 Ulm, Germany*
[10]*Core Facility Functional Peptidomics, Ulm University Medical Center, Meyerhofstr. 4, 89081 Ulm, Germany*

[11]These authors contributed equally

[12]Lead contact

*Correspondence: mhoffmann@dpz.eu (M.H.), spoehlmann@dpz.eu (S.P.)

SUMMARY

The global spread of SARS-CoV-2/COVID-19 is devastating health systems and economies worldwide. Recombinant or vaccine-induced neutralizing antibodies are used to combat the COVID-19 pandemic. However, the recently emerged SARS-CoV-2 variants B.1.1.7 (UK), B.1.351 (South Africa) and P.1 (Brazil) harbor mutations in the viral spike (S) protein that may alter virus-host cell interactions and confer resistance to inhibitors and antibodies. Here, using pseudoparticles, we show that entry of all variants into human cells is susceptible to blockade by the entry inhibitors soluble ACE2, Camostat, EK-1 and EK-1-C4. In contrast, entry of the B.1.351 and P.1 variant was partially (Casirivimab) or fully (Bamlanivimab) resistant to antibodies used for COVID-19 treatment. Moreover, entry of these variants was less efficiently inhibited by plasma from convalescent COVID-19 patients and sera from BNT162b2 vaccinated individuals. These results suggest that SARS-CoV-2 may escape neutralizing antibody responses, which has important implications for efforts to contain the pandemic.

INTRODUCTION

The pandemic spread of severe acute respiratory syndrome coronavirus 2 (SARS-CoV-2), the causative agent of coronavirus disease 2019 (COVID-19), is ravaging economies and health system worldwide and has caused more than 2.3 million deaths ((WHO), 2020). SARS-CoV-2, an enveloped, positive-strand RNA virus uses its envelope protein spike (S) to enter target cells and the viral and cellular factors involved in cell entry constitute targets for antiviral intervention.

Host cell entry depends on S protein binding to the cellular receptor ACE2 and S protein priming by the cellular serine protease TMPRSS2 (Hoffmann et al., 2020b; Zhou et al., 2020) and these processes can be disrupted by soluble ACE2 and serine protease inhibitors (Hoffmann et al., 2020b; Monteil et al., 2020; Zhou et al., 2020). The suitability of these agents for COVID-19 treatment is currently being evaluated within clinical trials. Further, the S protein of SARS-CoV-2 is the main target for neutralizing antibodies and several recombinant neutralizing antibodies, have been granted emergency use authorization (EUA) for COVID-19 treatment (Baum et al., 2020a; Chen et al., 2020). Finally, protective mRNA- and vector-based vaccines encoding the SARS-CoV-2 S protein have been approved for human use and are considered key to the containment of the COVID-19 pandemic (Baden et al., 2021; Polack et al., 2020).

The genetic information of SARS-CoV-2 has remained relatively stable after the detection of the first cases in Wuhan, China, in the winter season of 2019. The only exception was a D614G change in the viral S protein that became dominant early in the pandemic and that has been associated with increased transmissibility (Korber et al., 2020; Plante et al., 2020; Volz et al., 2021). In contrast, D614G has only a moderate impact on SARS-CoV-2 neutralization by sera from COVID-19 patients and by sera from vaccinated individuals (Korber et al., 2020; Weissman et al., 2021). In the recent weeks several SARS-CoV-2 variants emerged that seem to exhibit increased transmissibility. These variants harbor mutations in the viral S protein that may

compromise immune control, raising concerns that the rapid spread of these variants might undermine current efforts to control the pandemic.

The SARS-CoV-2 variant B.1.1.7 (UK variant), also termed variant of concern (VOC) 202012/01 or 20I/501Y.V1, emerged in the United Kingdom and was associated with a surge of COVID-19 cases (Kidd et al., 2021; Leung et al., 2021). Subsequently, spread of the B.1.1.7 variant in other countries was reported (Claro et al., 2021; Galloway et al., 2021; Surleac et al., 2021; Umair et al., 2021; Yadav et al., 2021). It harbors nine mutations in the S protein, six of which are located in the surface unit of the S protein, S1, and three are found in the transmembrane unit, S2 (Fig. 1). Exchange N501Y is located in the receptor binding domain (RBD), a domain within S1 that interacts with ACE2, and its presence was linked to increased human-human transmissibility (Leung et al., 2021; Zhao et al., 2021). Variants B.1.351 (501Y.V2, also termed South Africa variant, (Mwenda et al., 2021)) and P.1 (501Y.V3, also termed Brazil variant, (da Silva Francisco et al., 2021)) were also purported to be more transmissible and these variants harbor nine and eleven mutations in their S proteins, respectively, including three changes in the RBD, K417N/T, E484K and N501Y (Fig. 1) (CDC, 2021). However, it is largely unclear how the mutations present in the S proteins of B.1.1.7, B.1.351 and P.1 impact host cell interactions and susceptibility to entry inhibitors and antibody-mediated neutralization.

Here, we show that the S protein of the B.1.1.7, B.1.351 and P.1 variants mediate robust entry into human cell lines and that entry is blocked by soluble ACE2 (sACE2), protease inhibitors active against TMPRSS2 and membrane fusion inhibitors. In contrast, monoclonal antibodies with EUA for COVID-19 treatment partially or completely failed to inhibit entry driven by the S proteins of the B.1.351 and P.1 variants. Similarly, these variants were less efficiently inhibited by convalescent plasma and sera from individuals vaccinated with

BNT162b2. Our results suggest that SARS-CoV-2 variants B.1.351 and P.1 can evade inhibition by neutralizing antibodies.

RESULTS

The spike proteins of the SARS-CoV-2 variants mediate robust entry into human cell lines

We first investigated whether the S proteins of SARS-CoV-2 WT (Wuhan-1 isolate with D614G exchange), B.1.1.7, B.1.351 and P.1 variants (Fig. 1) mediated robust entry into cell lines. For this, we used a vesicular stomatitis virus (VSV)-based vector pseudotyped with the respective S proteins (Fig. S1A). This system faithfully mimics key aspects of SARS-CoV-2 entry into cells, including ACE2 engagement, priming of the S protein by TMPRSS2 and antibody-mediated neutralization (Hoffmann et al., 2020b; Riepler et al., 2020; Schmidt et al., 2020). The following cell lines are frequently used for SARS-CoV-2 research and were employed as target cells in our study: The African green monkey kidney cell line Vero, Vero cells engineered to express TMPRSS2, the human embryonic kidney cell line 293T, 293T cells engineered to express ACE2, the human lung cell line Calu-3 and the human colon cell line Caco-2. All cell lines tested express endogenous ACE2. In addition, Calu-3 and Caco-2 cells express endogenous TMPRSS2 (Bottcher-Friebertshauser et al., 2011; Kleine-Weber et al., 2018).

All S proteins studied were robustly expressed and mediated formation of syncytia in transfected cells (Fig. 2A). Entry into all cell lines was readily detectable (Fig. 2B and Fig. S1B). Particles bearing the S proteins of the SARS-CoV-2 variants entered 293T (P.1) and 293T-ACE2 (B.1.351 and P.1) cells with slightly reduced efficiency as compared to particles bearing WT S protein, while the reverse observation was made for Calu-3 cells (B.1.1.7). For the remaining cell lines, no significant differences in entry efficiency were observed (Fig. 2B). Collectively, these results indicate that the mutations present in the S proteins of the B.1.1.7, B.1.351 and P.1 variants are compatible with robust entry into human cells.

The spike proteins of the SARS-CoV-2 variants mediate fusion of human cells

The S protein of SARS-CoV-2 drives cell-cell fusion resulting in the formation of syncytia and this process might contribute to viral pathogenesis (Buchrieser et al., 2021). We employed a cell-cell fusion assay to determine whether the S proteins of the B.1.1.7, B.1.351 and P.1 variants drive fusion with human cells. For this, the S proteins were expressed in effector cells, which were subsequently mixed with target cells engineered to express ACE2 alone or in conjunction with TMPRSS2. The S protein of SARS-CoV was included as control. The SARS-CoV S protein failed to mediate fusion with target cells expressing only ACE2 but efficiently drove fusion with cells coexpressing ACE2 and TMPRSS2 (Fig. 3A-B), as expected (Hoffmann et al., 2020a). In contrast, the SARS-CoV-2 S protein mediated efficient membrane fusion in the absence of TMPRSS2 expression in target cells (Fig. 3A,B) again in keeping with expectations (Hoffmann et al., 2020a). Finally, the S proteins of all SARS-CoV-2 variants tested facilitated cell-cell fusion with similar (B.1.1.7) or slightly reduced (B.1.351 and P.1) efficiency as compared to WT S protein (Fig. 3A,B).

Similar stability and entry kinetics of particles bearing WT and variant S proteins

We next investigated whether the S proteins of the SARS-CoV-2 variants showed altered stability, which may contribute to the alleged increased transmissibility of the viral variants. For this, we incubated S protein-bearing particles for different time intervals at 33°C, a temperature that is present in the nasal cavity, and subsequently assessed their capacity to enter target cells. The efficiency of cell entry markedly decreased upon incubation of particles at 33°C for more than 8 h, but no appreciable differences were observed between particles bearing S proteins from SARS-CoV-2 WT or variants (Fig. 4A).

Although the S proteins of the SARS-CoV-2 variants did not differ markedly from WT S protein regarding stability and entry efficiency, they might mediate entry with different kinetics as compared to WT S protein. To investigate this possibility, we incubated target cells with S protein-bearing particles for the indicated time intervals, removed unbound virus by washing and universally determined entry efficiency at 16 h post inoculation. Entry efficiency increased with the time available for particle adsorption to cells but no differences were observed between particles bearing WT S protein or S protein from SARS-CoV-2 variants (Fig. 4B). Confirmation of the result with lung cells is pending. However, the data available at present indicate that there might be no major differences between WT SARS-CoV-2 and SARS-CoV-2 variants B.1.1.7, B.1.351 and P.1 regarding S protein stability and entry kinetics.

Soluble ACE2, TMPRSS2 inhibitors and membrane fusion inhibitors block entry

Soluble ACE2 (sACE2) blocks SARS-CoV-2 entry into cells and is in clinical development for COVID-19 therapy (Monteil et al., 2020). Similarly, the clinically proven protease inhibitors Camostat and Nafamostat block TMPRSS2-dependent SARS-CoV-2 cell entry and their potential for COVID-19 treatment is currently being assessed (Hoffmann et al., 2020b; Hoffmann et al., 2020c). Finally, the membrane fusion inhibitor EK-1 and its optimized lipid-conjugated derivative EK-1-C4 block SARS-CoV-2 entry by preventing conformational rearrangements in the S protein that are required for membrane fusion (Xia et al., 2020). We asked whether entry driven by the S proteins of the B.1.1.7, B.1.351 and P.1 variants can be blocked by these inhibitors. All inhibitors were found to be active although entry mediated by the S proteins of the SARS-CoV-2 variants was slightly more sensitive to blockade by sACE2 as compared to WT S protein (Fig. 5). In addition, entry driven by the S protein of the P.1 variant was slightly more sensitive to blockade by EK-1 and EK-1-C4 as compared to the other S proteins tested (Fig. 5).

These results suggest that sACE2, TMPRSS2 inhibitors and membrane fusion inhibitors will be active against the B.1.1.7, B.1.351 and P.1 variants.

Resistance against antibodies used for COVID-19 treatment

A cocktail of monoclonal antibodies (REGN-COV2, consisting of Casirivimab and Imdevimab) and the monoclonal antibody Bamlanivimab block SARS-CoV-2 WT infection (Fig. S2) and have received EUA for COVID-19 therapy. We analyzed whether these antibodies can inhibit entry driven by the S proteins of the B.1.1.7, B.1.351 and P.1 variants. Entry driven by the S proteins of all variants was comparably inhibited by Imdevimab while entry driven by the S proteins of the B.1.351 and P.1 variants was partially resistant against Casirivimab (Fig. 6). A cocktail of both antibodies (REGN-COV2) efficiently inhibited entry mediated by the S proteins of all variants. Finally, entry mediated by the S proteins of the B.1.351 and P.1 variant was completely resistant to REGN10989 and Bamlanivimab while the S protein of the B.1.1.7 variant was efficiently blocked by all antibodies tested (Fig. 6). Collectively, these data indicate that single antibodies with EUA might provide incomplete (Casirivimab) or no (Bamlanivimab) protection against the B.1.351 and P.1 variants.

Reduced neutralization by plasma from convalescent patients

SARS-CoV-2 infection can induce the production of neutralizing antibodies and these antibodies are believed to contribute to protection from reinfection (Rodda et al., 2020; Wajnberg et al., 2020). Therefore, it is important to elucidate whether B.1.1.7, B.1.351 and P.1 variants are efficiently neutralized by antibody responses in convalescent COVID-19 patients. We addressed this question using plasma collected from COVID-19 patients undergoing intensive care at Göttingen University Hospital, Germany (Table S1). The plasma samples had been pre-screened

for neutralizing activity against WT S protein, and a plasma sample with no neutralizing activity was included as negative control. Spread of SARS-CoV-2 variants in Germany was very limited at the time of sample collection, indicating that serum antibodies were induced in response to SARS-CoV-2 WT infection.

All plasma samples with known neutralizing activity (ID15, 18, 20, 22, 23, 24, 27, 33, 51) efficiently reduced entry driven by WT S protein while the control plasma (ID16) was inactive (Fig. 7A and Fig. S3). Blockade of entry driven by the S protein of the B.1.1.7 variant was slightly less efficient (Fig. 7A and Fig. S3). In contrast, seven out of nine plasma samples inhibited entry driven by the S proteins of the B.1.351 and P.1 variants less efficiently as compared to entry driven by WT S protein. These results suggest that individuals previously infected with WT SARS-CoV-2 might only be partially protected against infection with B.1.351 and P.1 variants of SARS-CoV-2.

Reduced neutralization by sera from BNT162b2-vaccinated individuals

The vaccine BNT162b2 is based on an mRNA that encodes for the viral S protein and is highly protective against COVID-19 (Polack et al., 2020). While the S protein harbors T-cell epitopes (Grifoni et al., 2020; Peng et al., 2020), efficient protection is believed to require the induction of neutralizing antibodies. We determined the neutralizing activity of sera from 15 donors immunized twice with BNT162b2 (Table S2). All sera efficiently inhibited entry driven by the WT S protein and inhibition of entry driven by the S protein of the B.1.1.7 variant was only slightly reduced (Fig. 7B and Fig. S3). In contrast, 12 out of 15 sera showed a markedly reduced inhibition of entry driven by the S proteins of the B.1.351 and P.1 variants (Fig. 7B), although it should be stated that all sera completely inhibited entry at the lowest dilution tested. In sum, these

results suggest that BNT162b2 may offer less robust protection against infection by the B.1.351 and P.1 variants as compared to SARS-CoV-2 WT.

DISCUSSION

The COVID-19 pandemic has taken a major toll on human health and prosperity. Non-pharmaceutic interventions are currently the major instrument to combat the pandemic but are associated with a heavy burden on economies. Protective vaccines became recently available and might become a game changer – it is hoped that efficient vaccine roll out might allow to attain herd immunity in certain countries in the second half of 2021. The recent emergence of SARS-CoV-2 variants B.1.1.7, B.1.351 and P.1 that harbor mutations in the major target of neutralizing antibodies, the viral S protein, raises the question whether vaccines available at present will protect against infection with these viruses. Similarly, it is largely unclear whether antibody responses in convalescent patients protect against re-infection with the new variants. The results of the present study suggest that SARS-CoV-2 variants B.1.351 and P.1 are partially (Casirivimab) or fully (Bamlanivimab) resistant against antibodies used for COVID-19 treatment and are inhibited less efficiently by convalescent plasma or sera from individuals immunized with the mRNA vaccine BNT162b2. These results suggest that strategies relying on antibody-mediated control of SARS-CoV-2 infection might be compromised by resistance development.

The increased transmissibility postulated for the B.1.1.7, B.1.351 and P.1 variants (da Silva Francisco et al., 2021; Leung et al., 2021; Mwenda et al., 2021) raises the possibility that these viruses might exhibit altered host-cell interactions or particle stability. The present study demonstrates that S proteins of SARS-CoV-2 WT, B.1.1.7, B.1.351 and P.1 mediate cell-cell and virus-cell fusion with roughly comparable efficiency and entry kinetics. Similarly, particles bearing S protein of WT and variant SARS-CoV-2 did not differ appreciably in stability although we cannot exclude that examination of more time points might have revealed minor differences. In keeping with these findings, entry driven by the S proteins of SARS-CoV-2 WT and variants was efficiently blocked by inhibitors targeting the cellular factors ACE2 and TMPRSS2, which

316 are critical for lung cell entry. Similarly, membrane fusion inhibitors blocked entry driven by WT
317 S protein and S proteins of the B.1.1.7, B.1.351 and P.1. variants with similar efficiency. These
318 results await confirmation with authentic virus and lung cells, in which entry kinetics might
319 differ. However, the data available at present do not point towards major differences in host cell
320 entry and stability of SARS-CoV-2 and variants B.1.1.7, B.1.351 and P.1.

321 Although host-cell interactions underlying viral entry might not differ markedly between
322 SARS-CoV-2 WT and the B.1.1.7, B.1.351 and P.1 variants, major differences in susceptibility to
323 antibody-mediated neutralization were observed. Entry driven by the S proteins of the B.1.351
324 and P.1 variants was only partially inhibited by Casirivimab (REGN10933), in keeping with
325 mutations present in the S protein of the B.1.351 and P.1 variants being located at the antibody
326 binding site (Fig. S2). Combining Casirivimab and Imdevimab (REGN10987) within an antibody
327 cocktail with EUA (REGN-COV2) restored efficient inhibition, suggesting that REGN-COV2
328 should be suitable for treatment of patients infected with variant B.1.351 or P.1. In contrast,
329 Bamlanivimab (Baum et al., 2020a; Baum et al., 2020b; Chen et al., 2020; Gottlieb et al., 2021),
330 another antibody with EUA for COVID-19 treatment, failed to block entry driven by the S
331 proteins of B.1.351 and P.1. This finding is in agreement with the E484K mutation being located
332 in the antibody binding site and suggests that Bamlanivimab should not be used for treatment of
333 patients infected with the B.1.351 and P.1 variants.

334 Vaccination is key to global efforts to contain the COVID-19 pandemic. The mRNA-
335 based vaccine BNT162b2 encodes the viral S protein and is highly efficacious. Closely related
336 vaccines as well as vector-based vaccines followed and it is believed that these vaccines mainly
337 protect by inducing neutralizing antibody responses. Similarly, neutralizing antibody responses
338 are believed to contribute to protection of convalescent COVID-19 patients against reinfection
339 and disease. The present study showed that entry driven by the S proteins of the B.1.351 and P.1

variants was less susceptible to inhibition by sera/plasma from COVID-19 patients and BNT162b2 vaccinated individuals as compared to entry driven by WT S protein. It should be noted that all plasma and sera tested completely inhibited entry at the lowest dilution tested and that T cell responses will contribute to control of SARS-CoV-2 infection, particularly in re-infected convalescent patients (Grifoni et al., 2020; Peng et al., 2020). Nevertheless, the markedly reduced sensitivity to antibody-mediated neutralization suggests that convalescent and vaccinated individuals might not be fully protected against infection by the B.1.351 and P.1 variants. Such a scenario would be in keeping with preliminary information suggesting that a vaccine based on the S protein might provide less effective protection in South Africa as compared to the US (Callaway and Mallapaty, 2021). On a more general level, our findings suggest that the interface between the SARS-CoV-2 S protein and ACE2 exhibits high plasticity, favoring emergence of escape variants.

Our finding that entry driven by the S protein of the B.1.1.7 variant can be efficiently inhibited by antibodies induced upon infection and vaccination is in agreement with those of Muik and colleagues, who reported that pseudoparticles bearing the B.1.1.7 S protein are efficiently neutralized by sera from BNT162b2 vaccinated individuals (Muik et al., 2021). Xie and coworkers found that authentic SARS-CoV-2 bearing two mutations present in the S protein of the B.1.1.7 variant (69/70-deletion + N501Y) was still robustly neutralized by antibodies induced by vaccination with BNT162b2. Similarly, neutralization of a virus bearing changes found in the RBD of the B.1.351 and P.1 variants (E484K + N501Y) was moderately reduced (Liu et al., 2021; Wang et al., 2021; Xie et al., 2021), again in keeping with our findings.

We present, to the best of our knowledge, the first side-by-side comparison of host cell entry of variants B.1.1.7, B.1.351 and P.1 and its inhibition by small molecules and antibodies. Although our results await confirmation with authentic SARS-CoV-2, they suggest that evasion

of antibody responses does not account for the rapid spread of B.1.1.7. In contrast, our findings indicate that the B.1.351 and P.1 variants might be able to spread in convalescent patients or BNT162b2 vaccinated individuals and thus constitute an elevated threat to human health. Containment of these variants by non-pharmaceutic interventions is an important task.

LIMITATIONS OF THE STUDY

Our study has the following limitations: We used vesicular stomatitis virus pseudotyped with the S proteins of SARS-CoV-2 variants to study SARS-CoV-2 entry and its inhibition. Although this surrogate model is believed to faithfully mimic cell entry of SARS-CoV-2, our results await formal confirmation with authentic virus. Furthermore, host cell entry and its blockade were studied using immortalized cell lines and these analyses should be extended to primary cell cultures within future studies.

ACKNOWLEDGMENTS

J.M. acknowledges funding by a Collaborative Research Centre grant of the German Research Foundation (316249678 – SFB 1279), the European Union's Horizon 2020 research and innovation programme under grant agreement No 101003555 (Fight-nCoV) and the Federal Ministry of Economics, Germany (Combi-CoV-2). J.M. and A.K. acknowledge funding by the Ministry for Science, Research and the Arts of Baden-Württemberg, Germany, and the German Research Foundation (Fokus-Förderung COVID-19). R.G. and A.S. are part of the International Graduate School in Molecular Medicine Ulm. S.P. acknowledges funding by BMBF (RAPID Consortium, 01KI1723D and 01KI2006D; RENACO, 01KI20328A; SARS_S1S2 01KI20396; COVIM consortium, 01KX2021), the county of Lower Saxony and the German Research Foundation (DFG) (PO 716/11-1, PO 716/14-1.) N.K. acknowledges funding from BMBF (ANI-CoV, 01KI2074A). H.S. acknowledges funding from the Ministry for Science, Research and the Arts of Baden-Württemberg, Germany and the European Commission (HORIZON2020 Project SUPPORT-E, no. 101015756). A.S.H. acknowledges funding from the German Research Foundation (HA 6013/6□1). We thank Lu Lu for advice with EK1 and EK1C4 synthesis.

AUTHOR CONTRIBUTIONS

Conceptualization, M.H., J.M., S.P.; Funding acquisition, S.P., J.M.; Investigation, M.H., P.A., R.G., A.S., B.F.H., A.S.H., N.K., L.G., H.H.-W., A.K., Essential resources, M.S.W., S.S., H.-M.J., B.J., H.S., M.M., A.K.; Writing, M.H. and S.P., Review and editing, all authors.

DECLARATION OF INTEREST

The authors declare not competing interests

REFERENCES

(WHO), W.H.O. (2020). Weekly epidemiological update - 9 February 2021 (WHO).

Baden, L.R., El Sahly, H.M., Essink, B., Kotloff, K., Frey, S., Novak, R., Diemert, D., Spector, S.A., Rouphael, N., Creech, C.B., *et al.* (2021). Efficacy and Safety of the mRNA-1273 SARS-CoV-2 Vaccine. N Engl J Med *384*, 403-416.

Bartosch, B., Dubuisson, J., and Cosset, F.L. (2003). Infectious hepatitis C virus pseudo-particles containing functional E1-E2 envelope protein complexes. J Exp Med *197*, 633-642.

Baum, A., Ajithdoss, D., Copin, R., Zhou, A., Lanza, K., Negron, N., Ni, M., Wei, Y., Mohammadi, K., Musser, B., *et al.* (2020a). REGN-COV2 antibodies prevent and treat SARS-CoV-2 infection in rhesus macaques and hamsters. Science *370*, 1110-1115.

Baum, A., Fulton, B.O., Wloga, E., Copin, R., Pascal, K.E., Russo, V., Giordano, S., Lanza, K., Negron, N., Ni, M., *et al.* (2020b). Antibody cocktail to SARS-CoV-2 spike protein prevents rapid mutational escape seen with individual antibodies. Science *369*, 1014-1018.

Berger Rentsch, M., and Zimmer, G. (2011). A vesicular stomatitis virus replicon-based bioassay for the rapid and sensitive determination of multi-species type I interferon. PLoS One *6*, e25858.

Bottcher-Friebertshauser, E., Stein, D.A., Klenk, H.D., and Garten, W. (2011). Inhibition of influenza virus infection in human airway cell cultures by an antisense peptide-conjugated morpholino oligomer targeting the hemagglutinin-activating protease TMPRSS2. J Virol *85*, 1554-1562.

Brass, A.L., Huang, I.C., Benita, Y., John, S.P., Krishnan, M.N., Feeley, E.M., Ryan, B.J., Weyer, J.L., van der Weyden, L., Fikrig, E., *et al.* (2009). The IFITM proteins mediate cellular resistance to influenza A H1N1 virus, West Nile virus, and dengue virus. Cell *139*, 1243-1254.

Brinkmann, C., Hoffmann, M., Lubke, A., Nehlmeier, I., Kramer-Kuhl, A., Winkler, M., and Pöhlmann, S. (2017). The glycoprotein of vesicular stomatitis virus promotes release of virus-like particles from tetherin-positive cells. PLoS One *12*, e0189073.

Buchrieser, J., Dufloo, J., Hubert, M., Monel, B., Planas, D., Rajah, M.M., Planchais, C., Porrot, F., Guivel-Benhassine, F., Van der Werf, S., *et al.* (2021). Syncytia formation by SARS-CoV-2-infected cells. EMBO J *40*, e107405.

Cai, Y., Zhang, J., Xiao, T., Peng, H., Sterling, S.M., Walsh, R.M., Jr., Rawson, S., Rits-Volloch, S., and Chen, B. (2020). Distinct conformational states of SARS-CoV-2 spike protein. Science *369*, 1586-1592.

Callaway, E., and Mallapaty, S. (2021). Novavax offers first evidence that COVID vaccines protect people against variants. Nature *590*, 17.

CDC, C.f.D.C.a.P. (2021). Emerging SARS-CoV-2 Variants.

Chen, P., Nirula, A., Heller, B., Gottlieb, R.L., Boscia, J., Morris, J., Huhn, G., Cardona, J., Mocherla, B., Stosor, V., *et al.* (2020). SARS-CoV-2 Neutralizing Antibody LY-CoV555 in Outpatients with Covid-19. N Engl J Med.

Claro, I.M., da Silva Sales, F.C., Ramundo, M.S., Candido, D.S., Silva, C.A.M., de Jesus, J.G., Manuli, E.R., de Oliveira, C.M., Scarpelli, L., Campana, G., *et al.* (2021). Local Transmission of SARS-CoV-2 Lineage B.1.1.7, Brazil, December 2020. Emerg Infect Dis *27*.

da Silva Francisco, R., Jr., Benites, L.F., Lamarca, A.P., de Almeida, L.G.P., Hansen, A.W., Gularte, J.S., Demoliner, M., Gerber, A.L., de, C.G.A.P., Antunes, A.K.E., *et al.* (2021). Pervasive transmission of E484K and emergence of VUI-NP13L with evidence of SARS-CoV-2 co-infection events by two different lineages in Rio Grande do Sul, Brazil. Virus Res, 198345.

Galloway, S.E., Paul, P., MacCannell, D.R., Johansson, M.A., Brooks, J.T., MacNeil, A., Slayton, R.B., Tong, S., Silk, B.J., Armstrong, G.L., *et al.* (2021). Emergence of SARS-CoV-2 B.1.1.7 Lineage - United States, December 29, 2020-January 12, 2021. MMWR Morb Mortal Wkly Rep *70*, 95-99.

Gottlieb, R.L., Nirula, A., Chen, P., Boscia, J., Heller, B., Morris, J., Huhn, G., Cardona, J., Mocherla, B., Stosor, V., *et al.* (2021). Effect of Bamlanivimab as Monotherapy or in Combination With Etesevimab on Viral Load in Patients With Mild to Moderate COVID-19: A Randomized Clinical Trial. JAMA.

464 Grifoni, A., Weiskopf, D., Ramirez, S.I., Mateus, J., Dan, J.M., Moderbacher, C.R., Rawlings,
465 S.A., Sutherland, A., Premkumar, L., Jadi, R.S., *et al.* (2020). Targets of T Cell Responses to
466 SARS-CoV-2 Coronavirus in Humans with COVID-19 Disease and Unexposed Individuals. Cell
467 *181*, 1489-1501 e1415.

468 Hansen, J., Baum, A., Pascal, K.E., Russo, V., Giordano, S., Wloga, E., Fulton, B.O., Yan, Y.,
469 Koon, K., Patel, K., *et al.* (2020). Studies in humanized mice and convalescent humans yield a
470 SARS-CoV-2 antibody cocktail. Science *369*, 1010-1014.

471 Heurich, A., Hofmann-Winkler, H., Gierer, S., Liepold, T., Jahn, O., and Pöhlmann, S. (2014).
472 TMPRSS2 and ADAM17 cleave ACE2 differentially and only proteolysis by TMPRSS2
473 augments entry driven by the severe acute respiratory syndrome coronavirus spike protein. J
474 Virol *88*, 1293-1307.

475 Hoffmann, M., Kleine-Weber, H., and Pöhlmann, S. (2020a). A Multibasic Cleavage Site in the
476 Spike Protein of SARS-CoV-2 Is Essential for Infection of Human Lung Cells. Mol Cell *78*, 779-
477 784 e775.

478 Hoffmann, M., Kleine-Weber, H., Schroeder, S., Kruger, N., Herrler, T., Erichsen, S.,
479 Schiergens, T.S., Herrler, G., Wu, N.H., Nitsche, A., *et al.* (2020b). SARS-CoV-2 Cell Entry
480 Depends on ACE2 and TMPRSS2 and Is Blocked by a Clinically Proven Protease Inhibitor. Cell
481 *181*, 271-280 e278.

482 Hoffmann, M., Muller, M.A., Drexler, J.F., Glende, J., Erdt, M., Gutzkow, T., Losemann, C.,
483 Binger, T., Deng, H., Schwegmann-Wessels, C., *et al.* (2013). Differential sensitivity of bat cells
484 to infection by enveloped RNA viruses: coronaviruses, paramyxoviruses, filoviruses, and
485 influenza viruses. PLoS One *8*, e72942.

486 Hoffmann, M., Schroeder, S., Kleine-Weber, H., Muller, M.A., Drosten, C., and Pöhlmann, S.
487 (2020c). Nafamostat Mesylate Blocks Activation of SARS-CoV-2: New Treatment Option for
488 COVID-19. Antimicrob Agents Chemother *64*.

489 Hornich, B.F., Grosskopf, A.K., Schlagowski, S., Tenbusch, M., Kleine-Weber, H., Neipel, F.,
490 Stahl-Hennig, C., and Hahn, A.S. (2021). SARS-CoV-2 and SARS-CoV spike-mediated cell-cell
491 fusion differ in the requirements for receptor expression and proteolytic activation. J Virol.

Jones, B.E., Brown-Augsburger, P.L., Corbett, K.S., Westendorf, K., Davies, J., Cujec, T.P., Wiethoff, C.M., Blackbourne, J.L., Heinz, B.A., Foster, D., *et al.* (2020). LY-CoV555, a rapidly isolated potent neutralizing antibody, provides protection in a non-human primate model of SARS-CoV-2 infection. bioRxiv.

Kidd, M., Richter, A., Best, A., Cumley, N., Mirza, J., Percival, B., Mayhew, M., Megram, O., Ashford, F., White, T., *et al.* (2021). S-variant SARS-CoV-2 lineage B1.1.7 is associated with significantly higher viral loads in samples tested by ThermoFisher TaqPath RT-qPCR. J Infect Dis.

Kleine-Weber, H., Elzayat, M.T., Hoffmann, M., and Pöhlmann, S. (2018). Functional analysis of potential cleavage sites in the MERS-coronavirus spike protein. Sci Rep *8*, 16597.

Kleine-Weber, H., Elzayat, M.T., Wang, L., Graham, B.S., Muller, M.A., Drosten, C., Pöhlmann, S., and Hoffmann, M. (2019). Mutations in the Spike Protein of Middle East Respiratory Syndrome Coronavirus Transmitted in Korea Increase Resistance to Antibody-Mediated Neutralization. J Virol *93*.

Korber, B., Fischer, W.M., Gnanakaran, S., Yoon, H., Theiler, J., Abfalterer, W., Hengartner, N., Giorgi, E.E., Bhattacharya, T., Foley, B., *et al.* (2020). Tracking Changes in SARS-CoV-2 Spike: Evidence that D614G Increases Infectivity of the COVID-19 Virus. Cell *182*, 812-827 e819.

Leung, K., Shum, M.H., Leung, G.M., Lam, T.T., and Wu, J.T. (2021). Early transmissibility assessment of the N501Y mutant strains of SARS-CoV-2 in the United Kingdom, October to November 2020. Euro Surveill *26*.

Liu, Y., Liu, J., Xia, H., Zhang, X., Fontes-Garfias, C.R., Swanson, K.A., Cai, H., Sarkar, R., Chen, W., Cutler, M., *et al.* (2021). Neutralizing Activity of BNT162b2-Elicited Serum - Preliminary Report. N Engl J Med.

Monteil, V., Kwon, H., Prado, P., Hagelkruys, A., Wimmer, R.A., Stahl, M., Leopoldi, A., Garreta, E., Hurtado Del Pozo, C., Prosper, F., *et al.* (2020). Inhibition of SARS-CoV-2 Infections in Engineered Human Tissues Using Clinical-Grade Soluble Human ACE2. Cell *181*, 905-913 e907.

519 Muik, A., Wallisch, A.K., Sanger, B., Swanson, K.A., Muhl, J., Chen, W., Cai, H., Maurus, D.,
520 Sarkar, R., Tureci, O., *et al.* (2021). Neutralization of SARS-CoV-2 lineage B.1.1.7 pseudovirus
521 by BNT162b2 vaccine-elicited human sera. Science.

522 Mwenda, M., Saasa, N., Sinyange, N., Busby, G., Chipimo, P.J., Hendry, J., Kapona, O., Yingst,
523 S., Hines, J.Z., Minchella, P., *et al.* (2021). Detection of B.1.351 SARS-CoV-2 Variant Strain -
524 Zambia, December 2020. MMWR Morb Mortal Wkly Rep *70*, 280-282.

525 Peng, Y., Mentzer, A.J., Liu, G., Yao, X., Yin, Z., Dong, D., Dejnirattisai, W., Rostron, T.,
526 Supasa, P., Liu, C., *et al.* (2020). Broad and strong memory CD4(+) and CD8(+) T cells induced
527 by SARS-CoV-2 in UK convalescent individuals following COVID-19. Nat Immunol *21*, 1336-
528 1345.

529 Plante, J.A., Liu, Y., Liu, J., Xia, H., Johnson, B.A., Lokugamage, K.G., Zhang, X., Muruato,
530 A.E., Zou, J., Fontes-Garfias, C.R., *et al.* (2020). Spike mutation D614G alters SARS-CoV-2
531 fitness. Nature.

532 Polack, F.P., Thomas, S.J., Kitchin, N., Absalon, J., Gurtman, A., Lockhart, S., Perez, J.L., Perez
533 Marc, G., Moreira, E.D., Zerbini, C., *et al.* (2020). Safety and Efficacy of the BNT162b2 mRNA
534 Covid-19 Vaccine. N Engl J Med.

535 Riepler, L., Rossler, A., Falch, A., Volland, A., Borena, W., von Laer, D., and Kimpel, J. (2020).
536 Comparison of Four SARS-CoV-2 Neutralization Assays. Vaccines (Basel) *9*.

537 Rodda, L.B., Netland, J., Shehata, L., Pruner, K.B., Morawski, P.A., Thouvenel, C.D., Takehara,
538 K.K., Eggenberger, J., Hemann, E.A., Waterman, H.R., *et al.* (2020). Functional SARS-CoV-2-
539 Specific Immune Memory Persists after Mild COVID-19. Cell.

540 Sauer, A.K., Liang, C.H., Stech, J., Peeters, B., Quere, P., Schwegmann-Wessels, C., Wu, C.Y.,
541 Wong, C.H., and Herrler, G. (2014). Characterization of the sialic acid binding activity of
542 influenza A viruses using soluble variants of the H7 and H9 hemagglutinins. PLoS One *9*,
543 e89529.

Schmidt, F., Weisblum, Y., Muecksch, F., Hoffmann, H.H., Michailidis, E., Lorenzi, J.C.C., Mendoza, P., Rutkowska, M., Bednarski, E., Gaebler, C., *et al.* (2020). Measuring SARS-CoV-2 neutralizing antibody activity using pseudotyped and chimeric viruses. J Exp Med *217*.

Surleac, M., Casangiu, C., Banica, L., Milu, P., Florea, D., Sandulescu, O., Streinu-Cercel, A., Vlaicu, O., Tudor, A., Hohan, R., *et al.* (2021). Evidence of novel SARS-CoV-2 variants circulation in Romania. AIDS Res Hum Retroviruses.

Umair, M., Ikram, A., Salman, M., Alam, M.M., Badar, N., Rehman, Z., Tamim, S., Khurshid, A., Ahad, A., Ahmad, H., *et al.* (2021). Importation of SARS-CoV-2 Variant B.1.1.7 in Pakistan. J Med Virol.

Volz, E., Hill, V., McCrone, J.T., Price, A., Jorgensen, D., O'Toole, A., Southgate, J., Johnson, R., Jackson, B., Nascimento, F.F., *et al.* (2021). Evaluating the Effects of SARS-CoV-2 Spike Mutation D614G on Transmissibility and Pathogenicity. Cell *184*, 64-75 e11.

Wajnberg, A., Amanat, F., Firpo, A., Altman, D.R., Bailey, M.J., Mansour, M., McMahon, M., Meade, P., Mendu, D.R., Muellers, K., *et al.* (2020). Robust neutralizing antibodies to SARS-CoV-2 infection persist for months. Science *370*, 1227-1230.

Wang, Z., Schmidt, F., Weisblum, Y., Muecksch, F., Barnes, C.O., Finkin, S., Schaefer-Babajew, D., Cipolla, M., Gaebler, C., Lieberman, J.A., *et al.* (2021). mRNA vaccine-elicited antibodies to SARS-CoV-2 and circulating variants. Nature.

Weissman, D., Alameh, M.G., de Silva, T., Collini, P., Hornsby, H., Brown, R., LaBranche, C.C., Edwards, R.J., Sutherland, L., Santra, S., *et al.* (2021). D614G Spike Mutation Increases SARS CoV-2 Susceptibility to Neutralization. Cell Host Microbe *29*, 23-31 e24.

Xia, S., Liu, M., Wang, C., Xu, W., Lan, Q., Feng, S., Qi, F., Bao, L., Du, L., Liu, S., *et al.* (2020). Inhibition of SARS-CoV-2 (previously 2019-nCoV) infection by a highly potent pan-coronavirus fusion inhibitor targeting its spike protein that harbors a high capacity to mediate membrane fusion. Cell Res *30*, 343-355.

Xie, X., Liu, Y., Liu, J., Zhang, X., Zou, J., Fontes-Garfias, C.R., Xia, H., Swanson, K.A., Cutler, M., Cooper, D., *et al.* (2021). Neutralization of SARS-CoV-2 spike 69/70 deletion, E484K and N501Y variants by BNT162b2 vaccine-elicited sera. Nat Med.

Yadav, P.D., Nyayanit, D.A., Sahay, R.R., Sarkale, P., Pethani, J., Patil, S., Baradkar, S., Potdar, V., and Patil, D.Y. (2021). Isolation and characterization of the new SARS-CoV-2 variant in travellers from the United Kingdom to India: VUI-202012/01 of the B.1.1.7 lineage. J Travel Med *28*.

Zhao, S., Lou, J., Cao, L., Zheng, H., Chong, M.K.C., Chen, Z., Chan, R.W.Y., Zee, B.C.Y., Chan, P.K.S., and Wang, M.H. (2021). Quantifying the transmission advantage associated with N501Y substitution of SARS-CoV-2 in the United Kingdom: An early data-driven analysis. J Travel Med.

Zhou, P., Yang, X.L., Wang, X.G., Hu, B., Zhang, L., Zhang, W., Si, H.R., Zhu, Y., Li, B., Huang, C.L., *et al.* (2020). A pneumonia outbreak associated with a new coronavirus of probable bat origin. Nature *579*, 270-273.

FIGURE LEGENDS

Figure 1. Schematic overview of the S proteins from the SARS-CoV-2 variants under study

The location of the mutations in the context of spike protein domain organization is shown in the upper panel. RBD = receptor binding domain, TD = transmembrane domain. The location of the mutations in the context of the trimer spike protein domain is shown lower panel. Color code: light blue = S1 subunit with RBD in dark blue, grey = S2 subunit, orange = S1/S2 and S2' cleavage sites, red = mutated amino acid residues.

Figure 2. S proteins from SARS-CoV-2 variants drive entry into human cell lines

(A) Directed expression of SARS-CoV-2 S proteins (SARS-2-S) in A549-ACE2 cells leads to the formation of syncytia. S protein expression was detected by immunostaining using an antibody directed against a C-terminal HA-epitope tag. Presented are the data from one representative experiment. Similar results were obtained in four biological replicates.

(B) The S proteins of the SARS-CoV-2 variants mediate robust entry into cell lines. The indicated cell lines were inoculated with pseudotyped particles bearing the S proteins of the indicated SARS-CoV-2 variants or wildtype (WT) SARS-CoV-2 S. Transduction efficiency was quantified by measuring virus-encoded luciferase activity in cell lysates at 16-20 h post transduction. Presented are the average (mean) data from six biological replicates (each conducted with technical quadruplicates). Error bars indicate the standard error of the mean (SEM). Statistical significance was analyzed by one-way analysis of variance (ANOVA) with Dunnett's posttest. See also Figure S1.

Figure 3. The S proteins of the SARS-CoV-2 variants drive robust cell-cell fusion

(A) Quantitative cell-cell fusion assay. S protein-expressing effector cells were mixed with ACE2 or ACE2/TMPRSS2 expressing target cells and cell-cell fusion was analyzed by measuring luciferase activity in cell lysates. Presented are the average (mean) data from four biological replicates (each performed with technical triplicates). Error bars indicate the SEM. Statistical significance was analyzed by one-way ANOVA with Dunnett's posttest.
(B) Qualitative fusion assay. A549-ACE2 (left) and A549-ACE2/TMPRSS2 (right) cells were transfected to express the indicated S proteins (or no viral protein) along with DsRed. At 24 h posttransfection, cells were fixed and analyzed for the presence of syncytia by fluorescence microscopy (magnification: 10x). Presented are representative images from a single experiment. Data were confirmed in three additional experiments.

Figure 4. Particles bearing the S proteins of SARS-CoV-2 variants exhibit similar stability and entry kinetics

(A) Particles bearing the indicated S proteins were incubated for different time intervals at 33 °C, snap frozen, thawed and inoculated onto Vero cells. Entry of particles that were frozen immediately was set as 100%.
(B) Particles bearing the indicated S proteins were incubated for indicated time intervals with Vero cells. Subsequently, the cells were washed and luciferase activity determined. Transduction measured without particle removal by washing was set as 100%.
For both panels, the average (mean) data from three biological replicates (each performed with technical quadruplicates) is presented. Error bars indicate the SEM. Statistical significance was analyzed by two-way ANOVA with Dunnett's posttest.

638 **Figure 5. Entry driven by the S proteins of the SARS-CoV-2 variants can be blocked with**
639 **soluble ACE2, protease inhibitors targeting TMPRSS2 and a membrane fusion inhibitor**
640 Top row, left panel: S protein-bearing particles were incubated with different concentrations of
641 soluble ACE2 (30 min, 37 °C) before being inoculated onto Caco-2 cells. Top row, middle and
642 right panel: Caco-2 target cells were pre-incubated with different concentrations of serine
643 protease inhibitor (Camostat or Nafamostat; 1 h, 37 °C) before being inoculated with particles
644 harboring the indicated S proteins. Bottom row, both panels: The peptidic fusion inhibitor EK-1
645 and its improved lipidated derivate EK-1-C4 were incubated with particles at indicated
646 concentrations (30 min, 37 °C) and then added to Caco-2 cells. All panels: Transduction
647 efficiency was quantified by measuring virus-encoded luciferase activity in cell lysates at 16-20 h
648 posttransduction. For normalization, inhibition of SARS-CoV-2 S protein-driven entry in samples
649 without soluble ACE2 or inhibitor was set as 0 %. Presented are the average (mean) data from
650 three biological replicates (each performed with technical triplicates [EK-1, EK-1-C4] or
651 quadruplicates [soluble ACE2, Camostat, Nafamostat]). Error bars indicate the SEM. Statistical
652 significance was analyzed by two-way ANOVA with Dunnett's posttest.
653

654 **Figure 6. Cell entry mediated by the S proteins of SARS-CoV-2 variants B.1.351 and P.1 is**
655 **partially or fully resistant to inhibition by monoclonal antibodies with EUA**
656 Pseudotypes bearing the indicated S proteins were incubated (30 min, 37 °C) with different
657 concentrations of control antibody (hIgG), four different monoclonal antibodies (Casirivimab,
658 Imdevimab, REGN10989, Bamlanivimab) or a combination of Casirivimab and Imdevimab, as
659 present in the REGN-CoV2 antibody cocktail, before being inoculated onto target Vero cells.
660 Transduction efficiency was quantified by measuring virus-encoded luciferase activity in cell
661 lysates at 16-20 h posttransduction. For normalization, inhibition of S protein-driven entry in

samples without antibody was set as 0 %. Presented are the data from a single experiment performed with technical triplicates. Data were confirmed in a separate experiment. Error bars indicate standard deviation (SD). See also Figure S2.

Figure 7. Entry driven by the S proteins of SARS-CoV-2 variants B.1.351 and P.1 shows reduces neutralization by convalescent plasma and sera from BNT162b2 vaccinated individuals

Pseudotypes bearing the indicated S proteins were incubated (30 min, 37 °C) with different dilutions of plasma derived from COVID-19 patients (A, see also Table S1) or serum from individuals vaccinated with the Pfizer/BioNTech vaccine BNT162b2 (obtained 13-15 days after the second dose) (B, see also Table S2) and inoculated onto Vero target cells. Transduction efficiency was quantified by measuring virus-encoded luciferase activity in cell lysates at 16-20 h posttransduction (please see Figure S3 for more details) and used to calculated the plasma/serum dilution factor that leads to 50% reduction in S protein-driven cell entry (neutralizing titer 50, NT50). Presented are the average (mean) NT50 from two independent experiments. The lines in the scatter plots indicate the median NT50, while the bars indicate the mean NT50. Identical plasma/serum samples are connected with lines in the bar graphs and the numbers in brackets indicate the average (mean) reduction in neutralization sensitivity for the S proteins of the respective SARS-CoV-2 variants. Statistical significance was analyzed by paired Student`s t-test.

686 ## Supplemental Figure Titles and Legends

687

688 **Figure S1. Graphical summary of the generation and use of VSV pseudotype particles**
689 **bearing SARS-2-S and representative transduction data (related to Figure 2)**

690 (A) Schematic illustration of how SARS-2-S-bearing VSV pseudotype particles are generated
691 and used for transduction experiments.

692 (B) Raw transduction data (cps, counts per second) from a representative experiment. Presented
693 are the data from a single representative experiment conducted with technical quadruplicates.
694 Error bars indicate the SD. Bald pseudotype particles bearing no viral glycoprotein and particles
695 harboring VSV-G served as negative (assay background) and positive controls, respectively.

696

697 **Figure S2. Location of SARS-2-S RBD mutations K417N/T, E484K and N501Y with respect**
698 **to the binding interface of the REGN-COV2 antibody cocktail (A) and the monoclonal**
699 **antibod Bamlanivimab (B) (related to Figure 6)**

700 The protein models of the SARS-2-S receptor-binding domain (RBD, blue) in complex with
701 antibodies Casirivimab (orange) and Imdevimab (green) were constructed based on the 6XDG
702 template (Hansen et al., 2020), while the protein models of the SARS-2-S RBD in complex with
703 antibody Bamlanivimab (purple) were based on the 7L3N template (Jones et al., 2020). Residues
704 highlighted in red indicate amino acid variations found in emerging SARS-CoV-2 variants.

705

706 **Figure S3. Representative neutralization data (related to Figure 7)**

707 Pseudotypes bearing the indicated S proteins were incubated (30 min, 37 °C) with different
708 dilutions of plasma derived from COVID-19 patients (A) or serum from individuals vaccinated
709 with the Pfizer/BioNTech vaccine BNT162b2 (obtained 13-15 days after the second dose) (B)

and inoculated onto Vero target cells. Transduction efficiency was quantified by measuring virus-encoded luciferase activity in cell lysates at 16-20 h posttransduction. Presented are the data from a single representative experiment conducted with technical triplicates (results were confirmed in a separate biological replicate). For normalization, inhibition of S protein-driven entry in samples without plasma/serum was set as 0 %. Error bars indicate the SD. The data were further used to calculated the plasma/serum dilution that leads to 50% reduction in S protein-driven cell entry (neutralizing titer, NT50, shown in Figure 7). Of note, serum BNT-10 was excluded from further analysis, as its extraordinary high neutralizing activity precluded a reliable NT50 determination.

STAR METHODS

RESOURCE AVAILABILITY

LEAD CONTACT

Requests for material can be directed to Markus Hoffmann (mhoffmann@dpz.eu) and the lead contact, Stefan Pöhlmann (spoehlmann@dpz.eu).

MATERIALS AVAILABILITY

All materials and reagents will be made available upon installment of a material transfer agreement (MTA).

DATA AND CODE AVAILABILITY

The study did not generate unique datasets or code.

EXPERIMENTAL MODEL AND SUBJECT DETAILS

Cell culture

All cell lines were incubated at 37 °C in a humidified atmosphere containing 5% CO2. All media were supplemented with 10% fetal bovine serum (FCS, Biochrom or GIBCO), 100 U/ml of penicillin and 0.1 mg/ml of streptomycin (PAN-Biotech). 293T (human, female, kidney; ACC-635, DSMZ, RRID: CVCL_0063), 293T cells stably expressing ACE2 (293T-ACE2), Vero (African green monkey, female, kidney; CRL-1586, ATCC, RRID:CVCL_0574; kindly provided by Andrea Maisner, Institute of Virology, Philipps University Marburg, Marburg, Germany) and Vero-TMPRSS2 cells (Hoffmann et al., 2020b) were cultivated in Dulbecco's modified Eagle

medium (DMEM). Vero-TMPRSS2 cells additionally received puromycin (0.5 µg/ml, Invivogen). A549 (human, male, lung; CRM-CCL-185, ATCC, RRID:CVCL_0023; kindly provided by Georg Herrler), A549-ACE2 and A549-ACE2/TMPRSS2 cells were cultivated in DMEM/F-12 Medium with Nutrient Mix (Thermo Fisher Scientific). A549-ACE2 cells further received 0.5 µg/ml puromycin, while A549-ACE2/TMPRSS2 cells were cultivated in the presence of 0.5 µg/ml puromycin and 1 µg/ml blasticidin. Caco-2 (human, male, intestine; HTB-37, ATCC, RRID:CVCL_0025) and Calu-3 cells (human, male, lung; HTB-55, ATCC, RRID:CVCL_0609; kindly provided by Stephan Ludwig, Institute of Virology, University of Münster, Germany) were cultivated in minimum essential medium supplemented with 1x non-essential amino acid solution (from 100x stock, PAA) and 1 mM sodium pyruvate (Thermo Fisher Scientific). 293T cells that stably express ACE2 were generated by retroviral (murine leukemia virus, MLV) transduction and selection of parental 293T cells with puromycin (4 µg/ml for initial selection and 0.5 µg/ml for sub-culturing). Similarly, we generated A549 cells stably expressing ACE2 (A549-ACE2). A549 cells stably expressing ACE2 and TMPRSS2 (A549-ACE2/TMPRSS2) were obtained by retroviral transduction of A549-ACE2 cells and selection with blasticidin (6 µg/ml for initial selection and 1 µg/ml for sub-culturing). Authentication of cell lines was performed by STR-typing, amplification and sequencing of a fragment of the cytochrome c oxidase gene, microscopic examination and/or according to their growth characteristics. Further, cell lines were routinely tested for contamination by mycoplasma.

METHODS DETAILS

Expression plasmids and transfection of cell lines

Expression plasmids for DsRed (Hoffmann et al., 2020b), vesicular stomatitis virus (VSV, serotype Indiana) glycoprotein (VSV-G) (Brinkmann et al., 2017), SARS-S (derived from the

Frankfurt-1 isolate; containing a C-terminal HA epitope tag) (Hoffmann et al., 2020b), SARS-2-S (codon-optimized, based on the Wuhan/Hu-1/2019 isolate; with a C-terminal truncation of 18 amino acid residues or with a C-terminal HA epitope tag) (Hoffmann et al., 2020b), angiotensin-converting enzyme 2 (ACE2) (Hoffmann et al., 2013), TMPRSS2 (Heurich et al., 2014), Gal4-TurboGFP-Luc and Vp16-Gal4 (Hornich et al., 2021) were previously described. have been described elsewhere. In order to generate expression vectors for S proteins from emerging SARS-CoV-2 variants, we introduced the required mutations into the parental SARS-2-S sequence by overlap extension PCR. Subsequently, the respective open reading frames were inserted into the pCG1 plasmid (kindly provided by Roberto Cattaneo, Mayo Clinic College of Medicine, Rochester, MN, USA), making use of the unique BamHI and XbaI restriction sites. Further, we cloned the coding sequence for human ACE2 into the pQCXIP plasmid (Brass et al., 2009), yielding pQCXIP_ACE2. For the generation of cell lines stably overexpressing human TMPRSS2 and/or human ACE2 we produced MLV-based transduction vectors using the pQCXIBl_cMYC-hTMPRSS2 (Kleine-Weber et al., 2018) or pQCXIP_ACE2 expression vectors in combination with plasmids coding for VSV-G and MLV-Gag/Pol (Bartosch et al., 2003). In order to obtain the expression vector for soluble human ACE2 harboring the Fc portion of human immunoglobulin G (sol-ACE2-Fc), we PCR amplified the sequence coding for the ACE2 ectodomain (amino acid residues 1-733) and cloned it into the pCG1-Fc plasmid ((Sauer et al., 2014), kindly provided by Georg Herrler, University of Veterinary Medicine, Hannover, Germany). Sequence integrity was verified by sequencing using a commercial sequencing service (Microsynth Seqlab). Specific cloning details (e.g., primer sequences and restriction sites) are available upon request. Transfection of cells was carried out by the calcium-phosphate method or by using polyethylenimin, Lipofectamine LTX (Thermo Fisher Scientific) or Transit LT-1 (Mirus).

804

805 **Analysis of S protein expression by fluorescence microscopy**

806 A549-ACE2 cells that were grown on coverslips were transfected with plasmids encoding SARS-
807 CoV-2 S protein variants with a C-terminal HA epitope tag or empty expression vector (control).
808 At 24 h posttransfection, cells were fixed with 4 % paraformaldehyde solution (30 min, room
809 temperature), washed and incubated (15 min, room temperature) with phosphate-buffered saline
810 (PBS) containing 0.1 M glycine and permeabilized by treatment with 0.2 % Triton-X-100
811 solution (in PBS, 15 min). Thereafter, samples were washed and incubated for 1 h at room
812 temperature with primary antibody (anti-HA, mouse, 1:500, Sigma-Aldrich) diluted in PBS
813 containing 1 % bovine serum albumin. Next, the samples were washed with PBS and incubated
814 in the dark for 1 h at 4 °C with secondary antibody (Alexa Fluor-568-conjugated anti-mouse
815 antibody, 1:750, Thermo Fisher Scientific). Finally, the samples were washed, nuclei were
816 stained with DAPI and coverslips were mounted onto microscopic glass slides with
817 Mowiol/DABCO. Images were taken using a Zeiss LSM800 confocal laser scanning microscope
818 with ZEN imaging software (Zeiss).

819

820 **Preparation of pseudotyped particles and transduction experiments**

821 Rhabdoviral pseudotype particles were prepared according to a published protocol (Kleine-
822 Weber et al., 2019). For pseudotyping we used a replication-deficient VSV vector that lacks the
823 genetic information for VSV-G and instead codes for two reporter proteins, enhanced green
824 fluorescent protein and firefly luciferase (FLuc), VSV∗ΔG-FLuc (kindly provided by Gert
825 Zimmer, Institute of Virology and Immunology, Mittelhäusern, Switzerland) (Berger Rentsch and
826 Zimmer, 2011). 293T cells transfected to express the desired viral glycoprotein were inoculated
827 with VSV∗ΔG-FLuc and incubated for 1 h at 37 °C before the inoculum was removed and cells

were washed. Finally, culture medium containing anti-VSV-G antibody (culture supernatant from I1-hybridoma cells; ATCC no. CRL-2700) was added. Following an incubation period of 16-18 h, pseudotype particles were harvested by collecting the culture supernatant, pelleting cellular debris through centrifugation (2,000 x g, 10 min, room temperature) and transferring aliquots of the clarified supernatant into fresh reaction tubes. Samples were stored at -80 °C. For transduction experiments, target cells were seeded in 96-well plates, inoculated with the respective pseudotype particles with comparable infectivity and further incubated. At 16-18 h postinoculation, transduction efficiency was analyzed. For this, the culture supernatant was removed and cells were lysed by incubation for 30 min at room temperature with Cell Culture Lysis Reagent (Promega). Next, lysates were transferred into white 96-well plates and FLuc activity was measured using a commercial substrate (Beetle-Juice, PJK; Luciferase Assay System, Promega) and a plate luminometer (Hidex Sense Plate Reader, Hidex or Orion II Microplate Luminometer, Berthold).

Depending on the experimental set-up target cells or pseudotype particles were pre-incubated with different compounds. Target cells were incubated with different concentrations of serine protease inhibitor (Camostat or Nafamostat, Caco-2, 1 h at 37 °C). Alternatively, pseudotype particles were pre-incubated with different concentrations of either sol-ACE2-Fc, fusion inhibitor (EK-1 or EK-1-C4), monoclonal antibodies (Casirivimab, Imdevimab, REGN-COV2 [Casirivimab and Imdevimab], REGN10989, Bamlanivimab), or plasma/sera from COVID-19 patients or vaccinated (Pfizer/BioNTech vaccine BNT162b2) individuals (30 min at 37 °C). S protein stability was analyzed as follows, pseudotype particles were incubated for different time intervals at 33 °C the snap-frozen and stored at -80 °C until all samples were collected. Thereafter, samples were thawed and inoculated onto target cells and incubated as described above. For the investigation of the entry speed of S protein-bearing pseudotypes, the

852 respective particles were inoculated on target cells and adsorbed for different time intervals
853 before the inoculum was removed and cells were washed and incubated with fresh medium.
854
855 **Production of soluble ACE2 (sol-ACE2-Fc)**
856 293T cells were grown in a T-75 flask and transfected with 20 µg of sol-ACE2-Fc expression
857 plasmid. At 10 h posttransfection, the medium was replaced and cells were further incubated for
858 38 h before the culture supernatant was collected and centrifuged (2,000 x g, 10 min, 4 °C). Next,
859 the clarified supernatant was loaded onto Vivaspin protein concentrator columns with a
860 molecular weight cut-off of 30 kDa (Sartorius) and centrifuged at 4,000 x g, 4 °C until the sample
861 was concentrated by a factor of 20. The concentrated sol-ACE2-Fc was aliquoted and stored at -
862 80 °C until further use.
863
864 **Collection of serum and plasma samples**
865 Sera from individuals vaccinated with BioNTech/Pfizer vaccine BNT162b2 were obtained 13-15
866 days after the second dose. The study was approved by the Ethic committee of Ulm university
867 (vote 31/21 – FSt/Sta). Collection of plasma samples from COVID-19 patients treated at the
868 intensive care unit was approved by the Ethic committee of the University Medicine Göttingen
869 (SeptImmun Study 25/4/19 Ü). For collection of plasma, Cell Preparation Tube (CPT)
870 vacutainers with sodium citrate were used and plasma was collected as supernatant over the
871 PBMC layer. For vaccinated patients, blood was collected in S-Monovette® Serum Gel tubes
872 (Sarstedt). Subsequently, the plasma and serum samples were incubated at 56°C for 30 min to
873 inactivate putative infectious virus and for convalescent plasma pre-screening for detection of
874 neutralizing activity was performed on Vero76 cells using SARS-2-S- and VSV-G bearing
875 pseudotypes as control, normalized for equal infectivity.

Qualitative cell-cell fusion assay

A549-ACE2 or A549-ACE2/TMPRSS2 cells were transfected with DsRed expression plasmid along with either expression vector for wildtype or mutant SARS-2-S, SARS-S or empty plasmid. At 24 h posttransfection, cells were fixed with 4 % paraformaldehyde solution (30 min, room temperature), washed and nuclei were stained with DAPI. Next, cells were washed again with PBS and images were taken using a Zeiss LSM800 confocal laser scanning microscope with ZEN imaging software (Zeiss).

Quantitative cell-cell fusion assay

293T target-cells were seeded in a 48-well plate at 50.000 cells/well and transfected with Gal4-TurboGFP-Luciferase expression plasmid (Gal4-TurboGFP-Luc) as well as expression plasmid for ACE2 alone or in combination with TMPRSS2 (7:1 ratio). 293T effector-cells were seeded in a 6-well dish at 70-80% confluency and transfected with the Vp16-Gal4 expression plasmid as well as expression plasmid for WT or mutant SARS-2-S, SARS-S or empty plasmid. At 24h posttransfection, effector-cells were detached by resuspending them in culture medium and added to the target-cells in a 1:1 ratio. After 24 h luciferase activity was analyzed using the Beetle-Juice Luciferase Assay according to manufacturer's instructions and a Biotek Synergy 2 plate reader.

Sequence analysis and protein models

S protein sequences of emerging SARS-CoV-2 S variants B.1.1.7 (EPI_ISL_601443), B.1.351 (EPI_ISL_700428) and B.1.1.28 (EPI_ISL_792683) were retrieved from the GISAID (global initiative on sharing all influenza data) database (https://www.gisaid.org/). Protein models are based on PDB: 6XDG (Hansen et al., 2020) or 7L3N (Jones et al., 2020), or a template generated

by modelling the SARS-2-S sequence on a published crystal structure (PDB: 6XR8,(Cai et al., 2020)), using the SWISS-MODEL online tool (https://swissmodel.expasy.org/), and were generated using the YASARA software (http://www.yasara.org/index.html).

QUANTIFICATION AND STATISTICAL ANALYSIS

The presented data either show (i) results from single representative experiment (conducted with technical triplicates or quadruplicates) that were confirmed in at least one additional biological replicate or (ii) average (mean) data from three or four biological replicates (conducted with technical triplicates or quadruplicates).

Data analysis was performed using Microsoft Excel as part of the Microsoft Office software package (version 2019, Microsoft Corporation) and GraphPad Prism 8 version 8.4.3 (GraphPad Software). Data normalization was done as follows: (i) To compare efficiency of cell entry driven by the different S protein variants under study, transduction was normalized against SARS-CoV-2 S WT (set as 100%); (ii) For experiments investigating inhibitory effects, transduction was normalized against a reference sample (e.g., control-treated cells or pseudotypes, set as 0% inhibition). Serum dilutions the cause a 50 % reduction of transduction efficiency (neutralizing titer 50, NT50), were calculated using a non-linear regression model (inhibitor vs. normalized response, variable slope). Statistical significance was tested by one- or two-way analysis of variance (ANOVA) with Dunnett's post-hoc test, or by paired student`s t-test. Only *P* values of 0.05 or lower were considered statistically significant ($P > 0.05$, not significant [ns]; $P \leq 0.05$, *; $P \leq 0.01$, **; $P \leq 0.001$, ***). Specific details on the statistical test and the error bars (standard deviation, SD; standard error of the mean, SEM) are indicated in the figure legends.

924 ## Supplemental Table Titles and Legends

925

926 **Table S1: COVID-19 patient data (related to Figure 7).**

927

928 **Table S2. BNT162b2-vaccinated patient data (related to Figure 7).** Serological data shows
929 antibody titer against Spike (IgG, IgA) and Nucleocapsid (NCP, IgG) protein measured by
930 Euroimmun-ELISA, values are given as baseline-corrected OD ratios compared to a calibrator.
931 For all analytes, a ratio < 0.8 was considered to be non-reactive or negative. An OD-ratio of ≥ 1.1
932 was considered to be positive for all three analytes.

933

SARS-CoV-2 variants B.1.351 and P.1 escape from neutralizing antibodies

Highlights:

- B.1.1.7, B.1.351 and P.1 do not show augmented host cell entry
- Entry inhibitors under clinical evaluation block all variants
- B.1.351 and P.1 can escape from therapeutic antibodies
- B.1.351 and P.1 evade antibodies induced by infection and vaccination

eTOC-Blurb:

Comparison of the SARS-CoV-2 variants B.1.1.7, B.1.351 and P.1 show that inhibitors under clinical evaluation are still effective in blocking entry though the B.1.351 and P.1 variants evade antibody responses induced upon infection as well as vaccination and evade certain therapeutic antibodies.

Figure 1

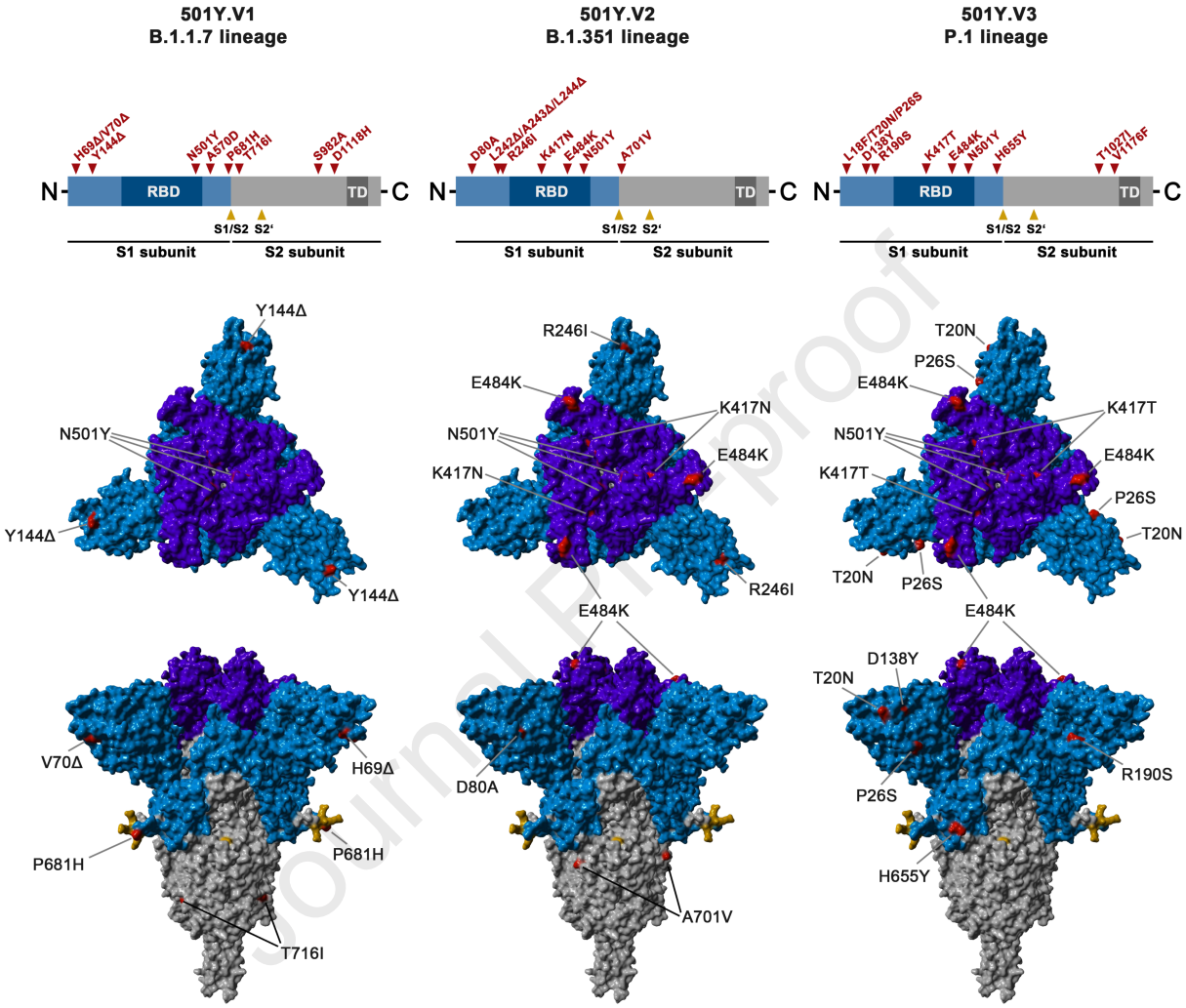

Figure 2

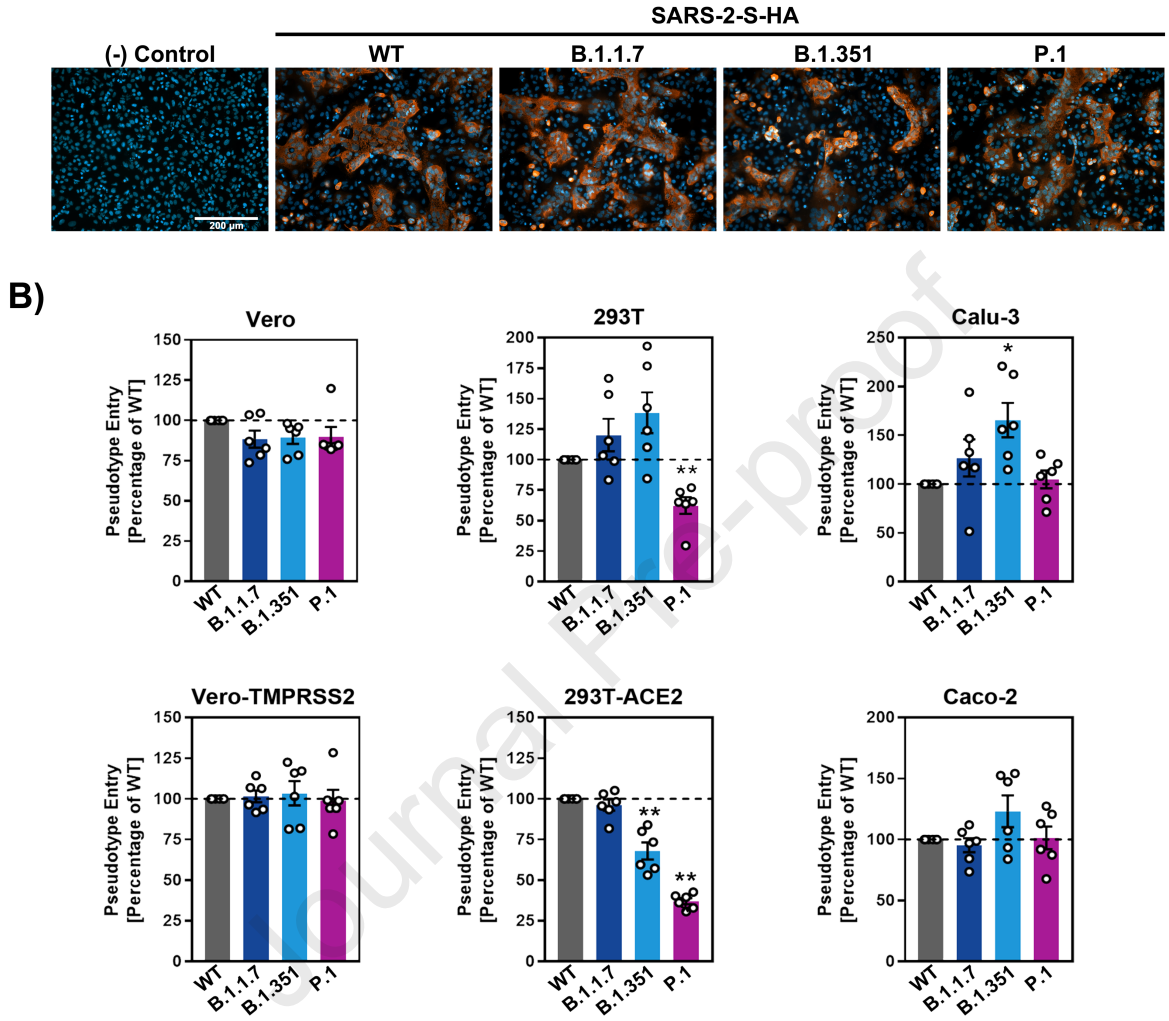

Figure 3

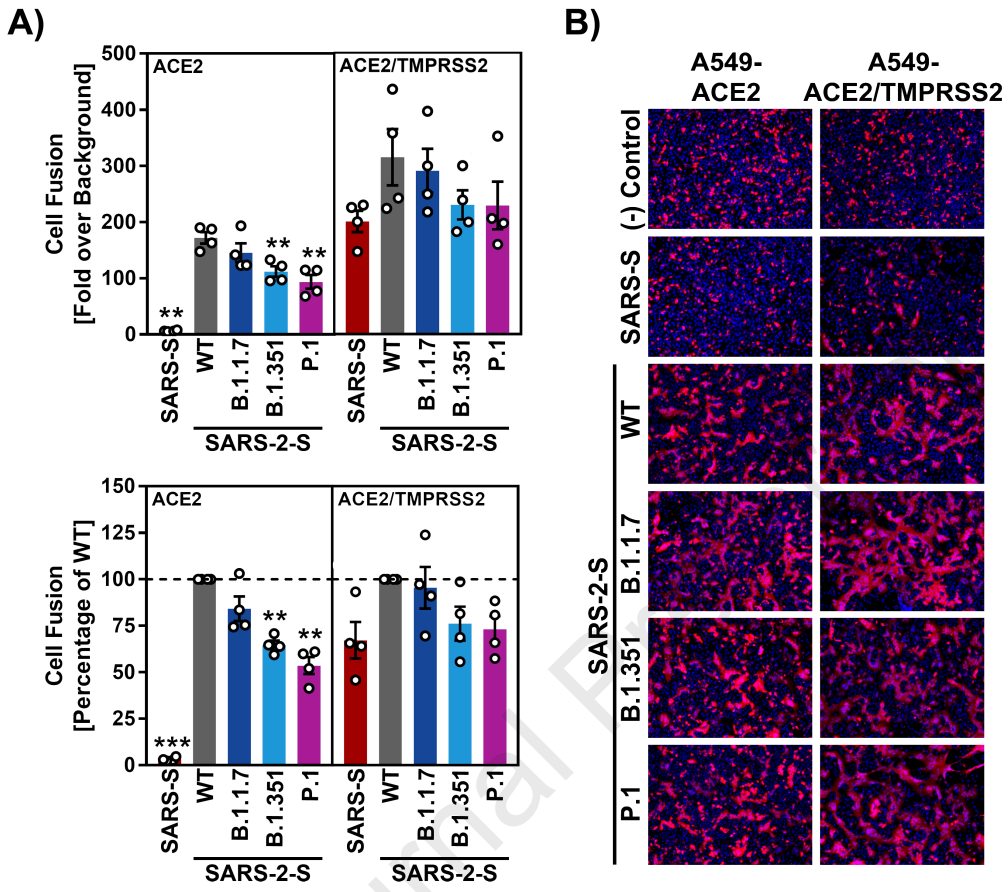

Figure 4

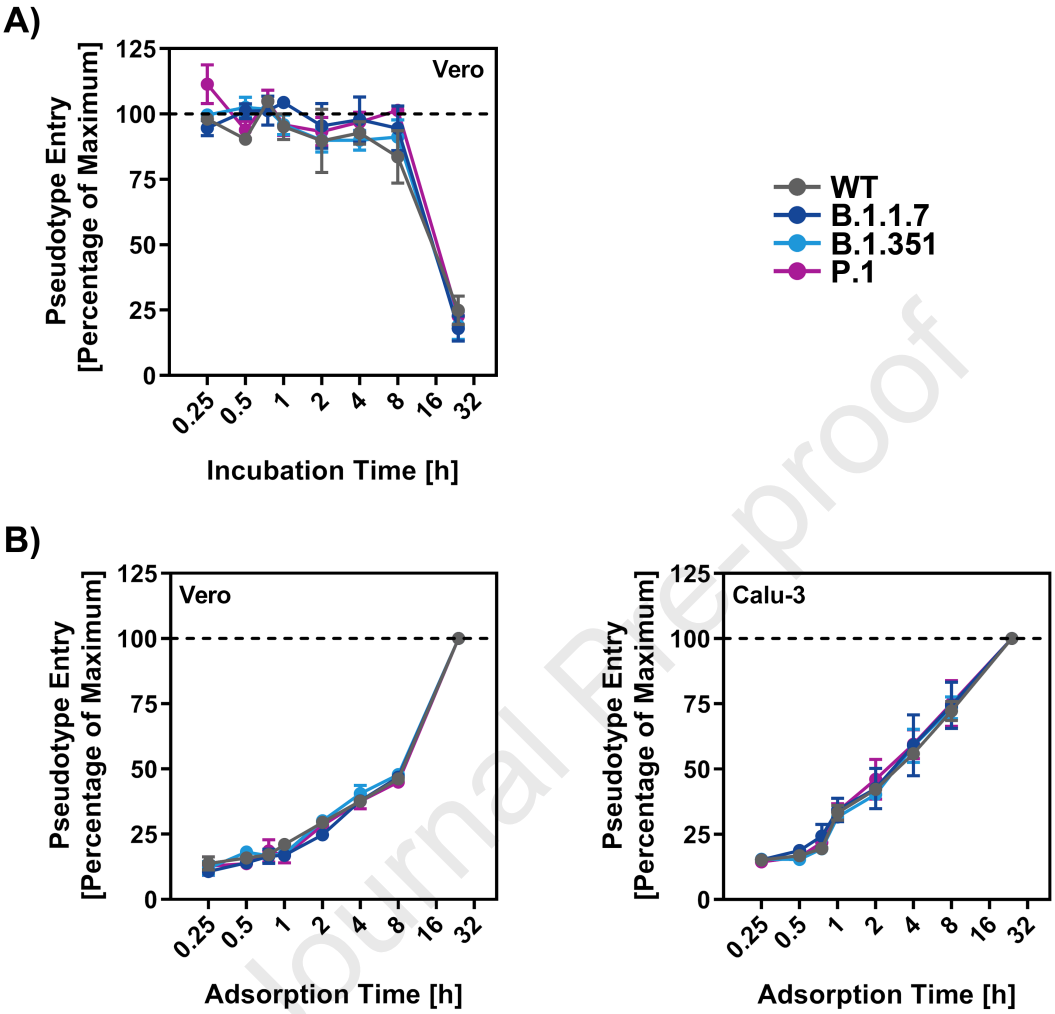

Figure 5

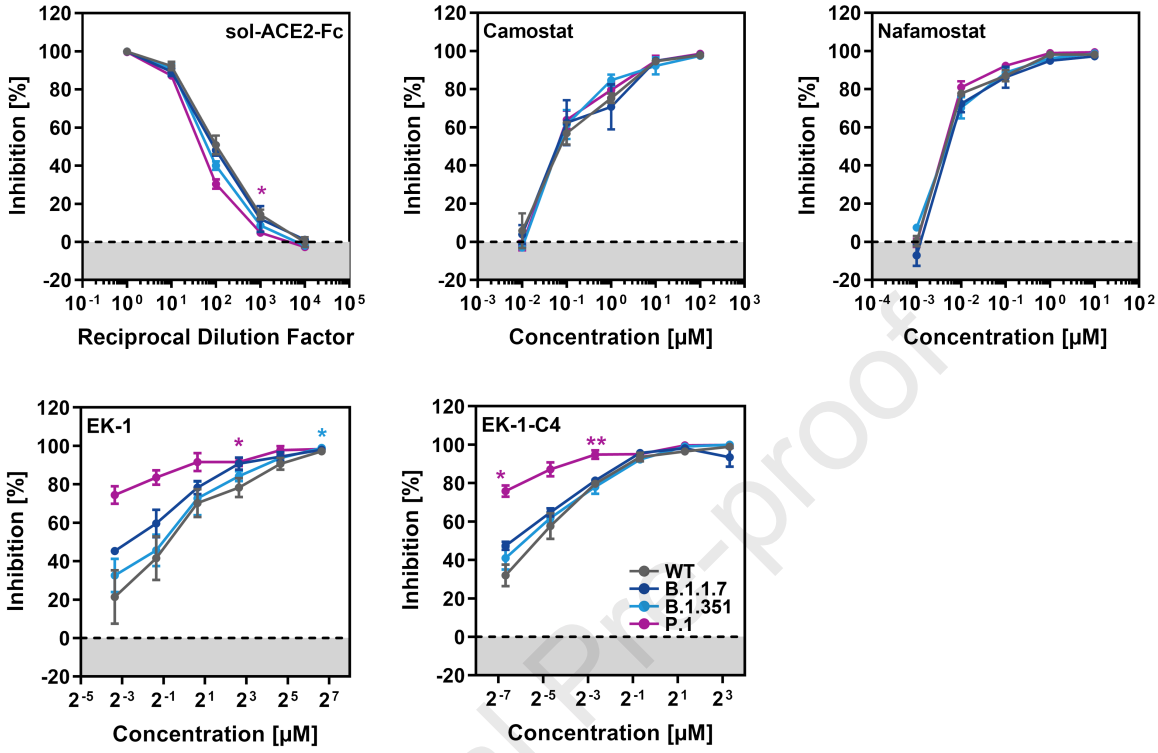

Figure 6

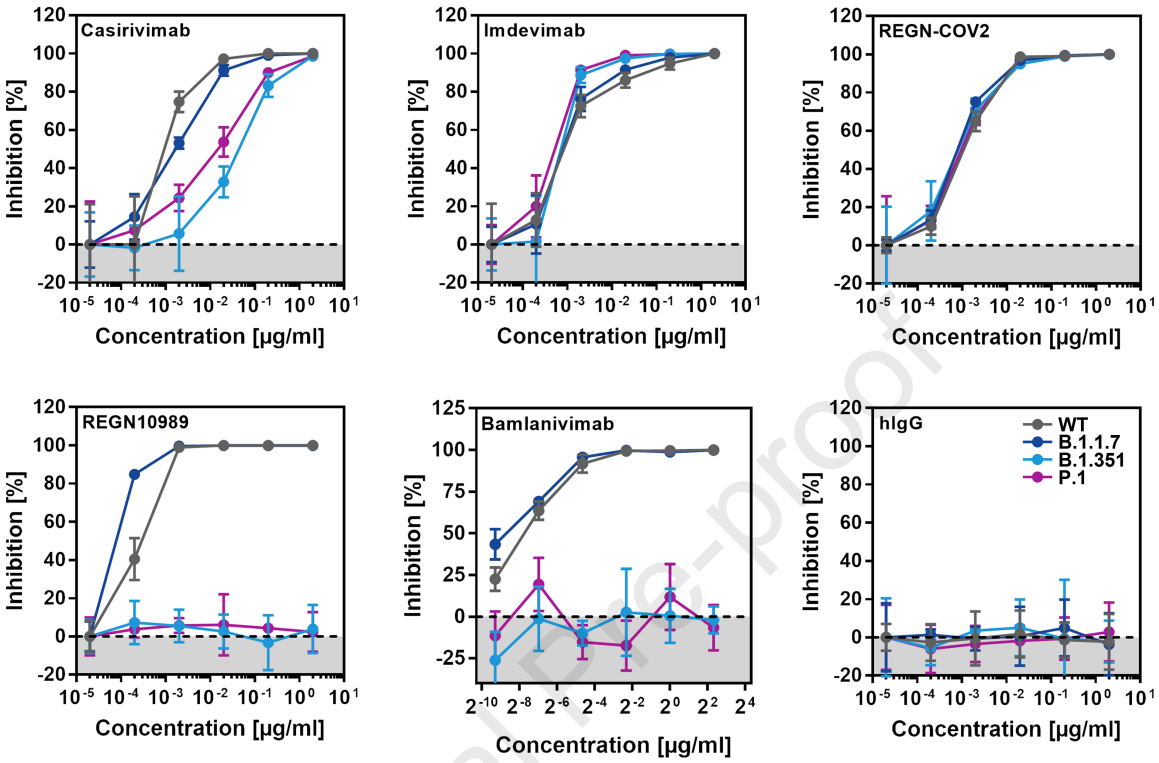

Figure 7